Acta Pharmacologica Sinica

www.nature.com/aps

ARTICLE

14-3-3ζ inhibits maladaptive repair in renal tubules by regulating YAP and reduces renal interstitial fibrosis

Tian-tian Wang[1], Ling-ling Wu[1], Jie Wu[1], Li-sheng Zhang[2], Wan-jun Shen[1], Ying-hua Zhao[1], Jiao-na Liu[1], Bo Fu[1], Xu Wang[1], Qing-gang Li[1], Xue-yuan Bai[1], Li-qiang Wang[3] and Xiang-mei Chen[1]

Acute kidney injury (AKI) refers to a group of common clinical syndromes characterized by acute renal dysfunction, which may lead to chronic kidney disease (CKD), and this process is called the AKI-CKD transition. The transcriptional coactivator YAP can promote the AKI-CKD transition by regulating the expression of profibrotic factors, and 14-3-3 protein zeta (14-3-3ζ), an important regulatory protein of YAP, may prevent the AKI-CKD transition. We established an AKI-CKD model in mice by unilateral renal ischemia-reperfusion injury and overexpressed 14-3-3ζ in mice using a fluid dynamics-based gene transfection technique. We also overexpressed and knocked down 14-3-3ζ in vitro. In AKI-CKD model mice, 14-3-3ζ expression was significantly increased at the AKI stage. During the development of chronic disease, the expression of 14-3-3ζ tended to decrease, whereas active YAP was consistently overexpressed. In vitro, we found that 14-3-3ζ can combine with YAP, promote the phosphorylation of YAP, inhibit YAP nuclear translocation, and reduce the expression of fibrosis-related proteins. In an in vivo intervention experiment, we found that the overexpression of 14-3-3ζ slowed the process of renal fibrosis in a mouse model of AKI-CKD. These findings suggest that 14-3-3ζ can affect the expression of fibrosis-related proteins by regulating YAP, inhibit the maladaptive repair of renal tubular epithelial cells, and prevent the AKI-CKD transition.

Keywords: 14-3-3ζ; YAP; acute kidney injury; AKI-CKD transition; ischemia-reperfusion injury; renal fibrosis

Acta Pharmacologica Sinica (2023) 44:381–392; https://doi.org/10.1038/s41401-022-00946-y

INTRODUCTION

Acute kidney injury (AKI) refers to a group of common clinical syndromes characterized by acute renal dysfunction and is also a common complication in critically ill patients that manifests as a rapid increase in creatinine and/or a decrease in the urine output [1]. Due to improvements in our understanding and the diagnosis of AKI, an increase in chronic diseases, and the wide application of contrast agents and nephrotoxic drugs, the incidence of AKI has increased significantly, and AKI has become a global public health problem [2, 3]. Previously, it was generally believed that the renal function of most patients could return to normal after AKI. However, in recent years, multiple studies have shown that many patients experience a continuous decline in renal function to varying degrees and present symptoms of chronic kidney disease (CKD), and this process is called the AKI-CKD transition [4, 5]. At present, there are no effective treatments for AKI, and symptomatic and supportive treatments such as glucocorticoid therapy, nutrition therapy and dialysis, which are often used in clinical practice, do not reduce the risk of AKI-CKD transition [6]. The maladaptive repair of renal tubular epithelial cell damage after AKI plays a central role in the AKI-CKD transition [7, 8]. After AKI, cell cycle arrest occurs, and transforming growth factor-β1 (TGF-β1) and other fibrogenic factors are synthesized and secreted in renal tubular epithelial cells. Activated TGF-β1 further promotes cell cycle arrest at the G_2/M phase, forming a vicious cycle that ultimately leads to the transformation of epithelial cells to myofibroblasts and promotes the AKI-CKD transition [9]. Therefore, reducing the damage to renal tubular epithelial cells, promoting their regeneration and repair, and inhibiting their transition to a fibrotic phenotype are keys to preventing the progression of AKI to CKD.

Kidney repair after AKI is related to various signaling pathways. Abnormalities in these pathways, including the Hippo axis, may have causal influences on the AKI-CKD transition. YAP is the most important transcriptional coactivator in the Hippo pathway and is involved in many physiological and pathological processes, including the regulation of organ volume, cell proliferation, differentiation, apoptosis, epithelial-mesenchymal transition, cell contact inhibition and maladaptive regeneration [10–12]. YAP is closely related to kidney fibrosis and is known as a profibrotic marker in studies of renal fibrosis [13]. YAP can promote the phenotypic transition of renal tubular epithelial cells to fibroblasts by regulating the transcription of key proteins in the signaling pathways related to fiber formation and participates in the process of renal fibrosis in mice with unilateral ureteral obstruction (UUO) [14]. Studies using multiple transgenic models in which YAP is

[1]Department of Nephrology, First Medical Center of Chinese PLA General Hospital, Nephrology Institute of the Chinese People's Liberation Army, State Key Laboratory of Kidney Diseases, National Clinical Research Center for Kidney Diseases, Beijing Key Laboratory of Kidney Disease Research, Beijing 100853, China; [2]College of Veterinary Medicine/College of Biomedicine and Health, Huazhong Agricultural University, Wuhan 430070, China and [3]Department of Ophthalmology, Chinese PLA General Hospital, Beijing 100853, China
Correspondence: Li-qiang Wang (liqiangw301@163.com) or Xiang-mei Chen (xmchen301@126.com)
These authors contributed equally: Tian-tian Wang, Ling-ling Wu

Received: 7 February 2022 Accepted: 30 May 2022
Published online: 15 July 2022

either deleted or hyperactivated have demonstrated the critical importance of YAP in driving progressive scarring in the kidney [15, 16]. Many scholars hold the view that inhibiting the activation of YAP is of great significance in the study of new strategies for the treatment of renal fibrosis [15, 17]. YAP may be involved in the maladaptive repair process of renal tubular epithelial cells and is expected to become a new target for inhibiting the AKI-CKD transition. YAP activity depends on its location in the cell. When YAP is phosphorylated, it cannot be translocated into the nucleus and remains in the cytoplasm, which inhibits its transcriptional regulatory activity. Phosphorylation at Ser127 is the main mechanism for the retention of YAP in the cytoplasm. 14-3-3 protein zeta (14-3-3ζ) encoded by gene tyrosine and tryptophan hydroxylase activator zeta (*YWHAZ*) promotes the phosphorylation of YAP and retains it protein in the cytoplasm by binding to YAP phosphorylated at the Ser127 site, which results in the inhibition of collagen deposition during skin remodeling in rats with deep burns and the promotion of dermal regeneration [18]. These results suggest that 14-3-3ζ can promote tissue regeneration and repair by regulating YAP.

This study focused on the ability of 14-3-3ζ to regulate the transcriptional coactivator YAP. The experimental studies consisted of the establishment of AKI-CKD in wild-type and 14-3-3ζ overexpressing mice and, of renal tubular epithelial cells with knockdown and overexpression of 14-3-3ζ. The aims of the study were to explore the effect and mechanism of 14-3-3ζ on the maladaptive repair of renal tubular epithelial cells after AKI and to transform these results into clinical applications.

MATERIALS AND METHODS

Establishment of animal models and specimen retention

SPF-grade C57BL/6 mice (male, aged 8 weeks, weighing 22 ± 2 g) were purchased from SPF Biotechnology Co. (Beijing China). Ischemia-reperfusion-induced AKI was established as previously described [19, 20]. Briefly, the animals were subjected to unilateral renal ischemia-reperfusion injury (UIRI) with renal pedicle clamping (FST, Foster City, CA, USA) for 40 min. Twenty days after UIRI, the contralateral intact kidney was uninephrectomized. The kidneys of the mice belonging to the sham operation group were exposed for 40 min without clamping of the blood vessels, and the remaining procedure was the same as that used for the model group. Serum and renal tissue were collected during sampling. All of the animal care and experimental procedures were approved by the Chinese PLA General Hospital Animal Care and Use Committee (2019-X15-65) and followed the guidelines for the Care and Use of Laboratory Animals published by the United States National Institutes of Health (NIH publication, 2011 Revision).

14-3-3ζ overexpression in vivo

14-3-3ζ was overexpressed in vivo using a plasmid-mediated method [21, 22]. The mice were divided into three groups: NC group, mice overexpressing the negative control plasmid and subjected to UIRI (UIRI + OE-NC); OE-14-3-3ζ group, mice overexpressing the 14-3-3ζ plasmid and subjected to UIRI (UIRI + OE-14-3-3ζ); and sham operation group. Three days after UIRI, a fluid dynamics-based gene transfection technique was used; that is, plasmids were injected into the mice through the tail vein. Subsequently, the mice belonging to the NC group and OE-14-3-3ζ groups were administered plasmid injections every 7 days. The animals were sacrificed 21 days later, and samples were collected.

Cell culture and treatment

In this experiment, human renal proximal tubular epithelial cells (HK-2 and HRPTEpiC) were cultured in medium containing 10% FBS at 37 °C in an incubator with 5% CO_2. HK-2 cells were purchased from ATCC (CRL-2190, Washington, DC, USA), and HRPTEpiC purchased from ScienCell Research Laboratories (Catalog #4100, Carlsbad, CA, USA) was isolated from human kidneys. To simulate ischemia-reperfusion injury, HK-2 cells were subjected to hypoxia-reoxygenation based on a previous study [23]. We administered TGF-β1 (10 ng/mL, PeproTech, Cranbury, NJ, USA) to human renal tubular epithelial cells (HK-2 and HRPTEpiC) to promote cell fibrosis in vitro.

Establishment of cell lines with 14-3-3ζ knockdown and overexpression

Cells were inoculated one day before transfection and transfected with siRNA or plasmid once the confluence of the cells in each well was approximately 60%. The siRNA transfection reagent was Lipofectamine RNAiMAX (Thermo Fisher Scientific, Waltham, MA, USA), and the plasmid transfection reagent was EndoFectin Max (GeneCopoeia, Guangzhou, China). Cells were collected for analysis of the mRNA level after 24 h and for protein analysis after 48 h. TGF-β1 treatment or hypoxia-reoxygenation was administered after 24 h in the intervention experiments.

The histopathological analysis, immunofluorescence staining and immunohistochemical staining

After the kidney tissues were fixed in 4% formaldehyde fixative for approximately 24 h, the tissues were dehydrated, waxed, and embedded to generate 4 μm-thick paraffin sections, which were stained with periodic acid-Schiff (PAS), Masson, and Sirius Red.

Histological changes due to tubular necrosis were quantitated by determining the percent of tubules that displayed cell necrosis, loss of brush border, cast formation, and tubule dilatation as follows: 0 = none, 1 = <10%, 2 = 11%–25%, 3 = 26%–45%, 4 = 46%–75%, and 5 = >76%. At least 5–10 fields (×200) from each slide were reviewed [24].

Immunofluorescence staining and immunohistochemical staining were performed using paraffin sectioning and microwave methods for antigen repair.

Biochemical tests

A BioAssay Systems creatinine test kit (DICT-500, Hayward, CA, USA) and urea test kit (DIUR-500) were used to detect serum creatinine and urea nitrogen levels in mice according to the product manuals.

Western blotting

The primary antibody diluent was prepared with 1:50 blocking solution (casein solution) according to the instructions provided with the purchased antibody: mouse anti-GAPDH (1:10000, Proteintech, Rosemont, IL, USA), rabbit anti-14-3-3ζ (1:1000, Novus Biologicals, Littleton, CO, USA), rabbit anti-p-YAP (Ser127) (1:1000, Cell Signaling Technology, Danvers, MA, USA), rabbit anti-active YAP (1:1000, Abcam, Cambridge, UK), rabbit anti-CTGF (1:1000, Abcam), rabbit anti-α-SMA (1:500, Abcam), rabbit anti-vimentin (1:1000, Abcam), and goat anti-E-cadherin (1:400, R&D, Minneapolis, MN, USA). The detailed information of antibodies is presented in Supplementary Table S1. The transferred nitrocellulose filter membranes (NC membrane) were blocked with 1:20 casein solution for 2 h at room temperature and incubated with the primary antibody overnight at 4 °C. After washing with Tris-buffered saline Tween-20 (TBST), the NC membranes were incubated with the following secondary antibodies with 1:50 blocking solution: goat anti-mouse (1:1000, Beyotime, Shanghai, China), goat anti-rabbit (1:1000, Beyotime), and donkey anti-goat (1:1000, Beyotime). The NC membranes were detected after another wash with TBST.

Coimmunoprecipitation

Cell protein was extracted, and a small amount of supernatant was denatured and used in the input experiment. IgG (1.0 μg) and 20 μL of protein A/G beads were added to the supernatant of the negative control (IgG) proteins. Twenty microliters of protein A/G beads were added to the experimental groups. The cells were shaken at 4 °C

Table 1. Primer sequences for qRT-PCR

Gene	Forward (5′-3′)	Reverse (5′-3′)
18S	GTAACCCGTTGAACCCCATT	CCATCCAACGGTAGTAGCG
YWHAZ	CCTGCATGAAGTCTGTAACTGAG	GACCTACGGGCTCCTACAACA
Ywhaz	TGAGCTGTCGAATGAGGAGAG	CCTCCACGATGACCTACGG
Yap	ACCCTCGTTTTGCCATGAAC	TTGTTTCAACCGCAGTCTCTC
Ccn	GGCCTCTTCTGCGATTTCG	GCAGCTTGACCCTTCTCGG
Acta2	CCCAGACATCAGGGAGTAATGG	TCTATCGGATACTTCAGCGTCA
Col1a1	AGCAGACGGGAGTTTCTCCT	AGCTGACTTCAGGGATGTCTTC

and incubated for 1 h, and the supernatant was collected after centrifugation. The antibodies were added and incubated overnight at 4 °C. After the addition of 80 μL of protein A/G beads, the mixture was incubated at 4 °C for 2 h; subsequently, the supernatant after centrifugation was carefully absorbed to collect immunoprecipitation complexes. The immunoprecipitation complexes were then washed four times with 1 mL of precooled IP lysate, and after discarding the supernatant, 80 μL of 1× Sample Loading Buffer was added. The mixture was then boiled for 10 min in boiling water and the centrifuged, and the supernatant was collected for IB detection. The primary antibodies were rabbit anti-YAP (1:1000, Cell Signaling Technology) and mouse anti-14-3-3ζ (1:1000, Abcepta, San Diego, CA, USA).

qRT-PCR

Cellular mRNA was collected using the TRIzol method. A First Strand cDNA Synthesis Kit (NEB, Ipswich, MA, USA) was used for reverse transcription. The qRT-PCR system was established following the instructions provided with the SYBR Select Master Mix (Thermo Fisher Scientific). The primer sequences are presented in Table 1.

Statistical analysis

The data from more than 3 independent experiments are shown as scatter plots with bars and were analyzed by an unpaired *t* test or one-way ANOVA using SPSS Statistics 23 software. Differences with $P < 0.05$ were considered significant.

RESULTS

The expression of 14-3-3ζ was higher at the AKI stage and returned to normal at the CKD stage

We established an AKI-CKD model using the UIRI method. The changes in serum biochemical indicators, pathological PAS staining, Masson staining, Sirius Red staining and pathological scoring results revealed the successful establishment of the AKI-CKD model in mice (Supplementary Fig. S1). qRT-PCR results showed that the expression of 14-3-3ζ at the mRNA level increased gradually to the AKI stage and had returned to the normal levels at the CKD stage (Fig. 1a). Western blotting results revealed that the expression of 14-3-3ζ exhibited a time-dependent increase similar to the results found for the gene levels at the AKI stage, although its expression at each time point in the CKD stage was lower than that at the AKI stage. Anti-active YAP antibody (Abcam, ab205270) is specific to the active (nonphosphorylated) form of YAP, which showed a significant increase during the AKI-CKD transition; the expression levels of the fibrotic markers α-SMA and vimentin at 24 h, 48 h and 72 h were not significantly different from those of the sham group, and their expression levels were significantly higher at two time points in the CKD stage (Fig. 1b and c). The immunofluorescence staining results showed that the expression of 14-3-3ζ was increased at the AKI stage, peaked at 72 h, and then decreased to normal levels at the CKD stage. To determine the localization of 14-3-3ζ, we performed costaining with proliferating cell nuclear antigen (PCNA), which is an important marker protein of cell proliferation and is mainly expressed in renal tubular epithelial cells that proliferate or repair after injury. The costaining results showed that a few proliferating cells were observed after 24 h in the AKI stage, and many PCNA-positive cells appeared in the renal tubules at 72 h. The trend found for 14-3-3ζ expression was consistent with that found for PCNA. Both 14-3-3ζ and PCNA were expressed in renal tubular epithelial cells (Fig. 1d). In summary, the expression of 14-3-3ζ was higher at the AKI stage and tended to return to normal levels at the CKD stage. Therefore, we hypothesized that 14-3-3ζ can inhibit fibrillogenesis and slow the AKI-CKD transition.

The knockdown or overexpression of 14-3-3ζ caused changes in phosphorylated YAP (p-YAP) and active YAP

14-3-3ζ (Homo) siRNA was constructed by GenePharma (Suzhou, China), and the 14-3-3ζ (Homo) overexpression plasmid was constructed by GeneCopoeia (Fig. 2a and Table S2). HK-2 cells were transfected with 14-3-3ζ siRNA (si-14-3-3ζ group), 14-3-3ζ overexpression plasmid (OE-14-3-3ζ group) or their respective negative controls (NC group). qRT-PCR results showed that 14-3-3ζ mRNA expression was significantly reduced in the si-14-3-3ζ group and increased in the OE-14-3-3ζ group compared to with the levels in the NC group (Fig. 2b and c). Western blotting results showed that 14-3-3ζ knockdown decreased the intracellular p-YAP levels and increased the active YAP levels (Fig. 2d and e). In contrast, the overexpression of 14-3-3ζ led to an increase in p-YAP expression and a decrease in active YAP expression at the protein level (Fig. 2f and g). Co-IP experiments were performed to verify the interaction between YAP and 14-3-3ζ. The results showed that YAP could combine with 14-3-3ζ in renal tubular epithelial cells (Fig. 2h).

14-3-3ζ maintained the homeostasis of renal tubular epithelial cells and promoted their proliferation and repair after hypoxia-reoxygenation

We used Click-iT Plus EdU Imaging Kits (Thermo Fisher Scientific) to detect the proliferation of HK-2 cells, and the EdU-positive rate reflected the proliferation rate of the different groups. Compared with the NC group, the proliferation of the si-14-3-3ζ group was significantly lower, whereas that of the OE-14-3-3ζ group was unchanged (Fig. 3a and b). To test the ability of 14-3-3ζ to promote the proliferation of renal tubular epithelial cells and inhibit their maladaptive repair, we subjected each group of cells to hypoxia-reoxygenation. The OE-14-3-3ζ group exhibited more obvious proliferation and repair ability after injury, but the same finding was not found for the si-14-3-3ζ group (Fig. 3c and d).

14-3-3ζ alleviated the expression of fibrosis-related proteins induced by TGF-β1

TGF-β1 is a recognized means for promoting cell fibrosis in vitro [25]. In this study, we administered TGF-β1 to human renal tubular epithelial cells (HK-2 and HRPTEpiC) with 14-3-3ζ knockdown or overexpression. The concentration of TGF-β1 added to the complete medium was 10 ng/mL. Cells were collected 48 h after the stimulus was applied. Western blotting revealed that the active YAP levels in the cells of the si-14-3-3ζ group was significantly higher, the expression of the fibrotic marker proteins α-SMA and vimentin was further increased, and the expression of the epithelial cell marker protein E-cadherin was further down-regulated (Fig. 4a and b). Immunofluorescence staining showed that E-cadherin was mainly expressed on the membrane and cytoplasm of HRPTEpiC cells, and α-SMA was mainly located in the intercellular space. The quantitative changes in the expression of E-cadherin and α-SMA were consistent with the Western blotting results (Fig. 4c and d). The OE-14-3-3ζ group yielded the opposite Western blotting and immunofluorescence results (Fig. 5). The overexpression of 14-3-3ζ inhibited the phenotypic transition of renal tubular epithelial cells to myofibroblasts.

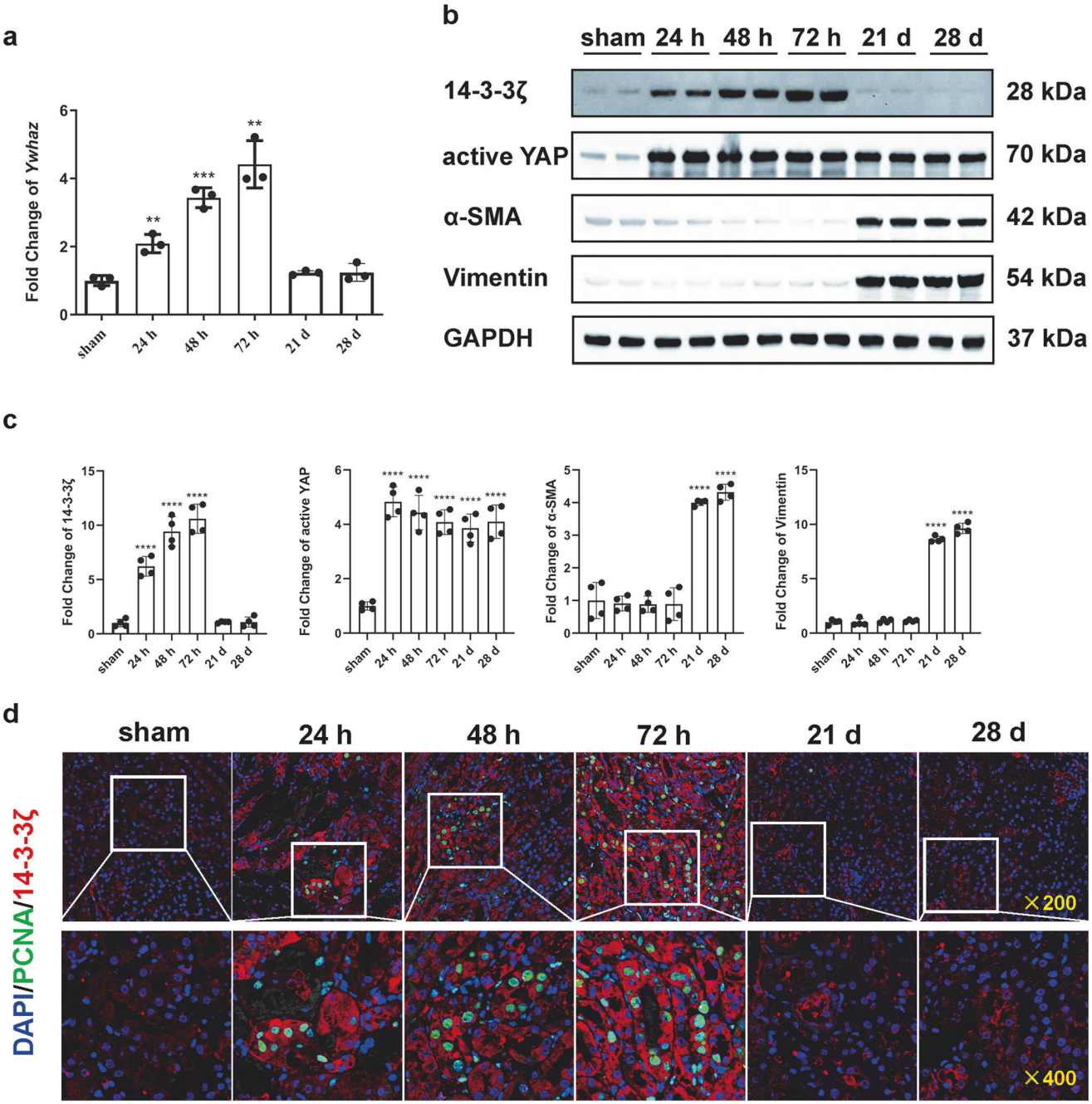

Fig. 1 The expression of 14-3-3ζ was increased at the AKI stage and returned to normal levels at the CKD stage in the AKI-CKD model. **a** qRT-PCR results showed that the expression of *Ywhaz* at the mRNA level increased gradually to the AKI stage but returned to normal levels at the CKD stage. $^{**}P < 0.01$ and $^{***}P < 0.001$ versus the sham group, $n = 3$. **b**, **c** The expression of 14-3-3ζ and related proteins was quantitatively detected by Western blotting. 14-3-3ζ expression was increased at the AKI stage and then decreased at the CKD stage. This trend was similar to that found for its mRNA expression level. Active YAP was always maintained at high expression levels. The levels of the fibrotic markers α-SMA and vimentin was not significantly changed at the AKI stage but was significantly increased at the CKD stage. $^{****}P < 0.0001$ versus the sham group, $n = 4$. **d** The expression of PCNA and 14-3-3ζ increased in tubular epithelial cells repaired after injury at the AKI stage and then declined at the CKD stage. The magnification of the original and enlarged images is ×200 and ×400, respectively.

14-3-3ζ was overexpressed in a mouse model of AKI-CKD by plasmid transfection

For further in vivo experiments aiming to observe the effect of 14-3-3ζ overexpression in AKI-CKD model mice, we constructed 14-3-3ζ (Mus) overexpression plasmids (Fig. 6b and Table S2) and transfected them into a mouse model of AKI-CKD using hydrodynamic-based transfection technology. The detailed experimental procedure is as follows: Three days after UIRI and every 7 days, 14-3-3ζ plasmids were transfected into the OE-14-3-3ζ group via tail vein injection, and NC plasmids were injected into the NC group. The samples were collected 21 days after establishment of the models (Fig. 6a). Using the immunofluorescence method, 10 fields of view were randomly selected from each sample under a 400-fold field of view, and the transfection efficiency was calculated based on the proportion of 14-3-3ζ-positive areas. The average transfection efficiency was 26.57% (Fig. 6c). qRT-PCR results showed changes in *Yap* and its downstream factors. Interestingly, *Yap* did not change

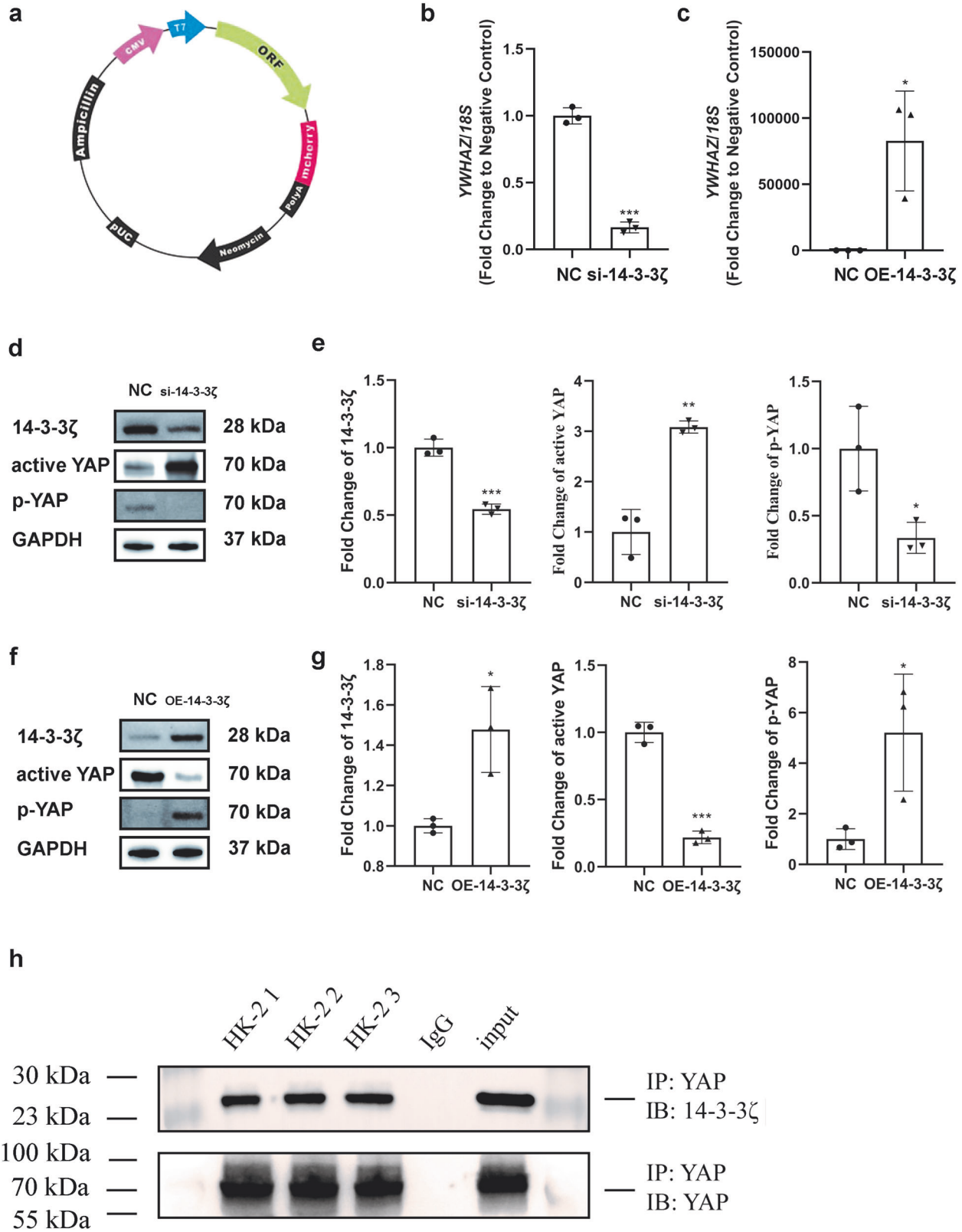

Fig. 2 14-3-3ζ was efficiently knocked down or overexpressed in HK-2 cells. a The construction of the 14-3-3ζ (Homo) plasmid was performed by GeneCopoeia. **b**, **c** *YWHAZ* was knocked down and overexpressed at the mRNA level in HK-2 cells. $^{*}P < 0.05$ and $^{***}P < 0.001$ versus the sham group, $n = 3$. **d**–**g** After 14-3-3ζ knockdown, the expression of p-YAP was decreased, and the expression of active YAP was increased. However, the in vitro overexpression of 14-3-3ζ yielded the opposite effect. $^{*}P < 0.05$, $^{**}P < 0.01$, and $^{***}P < 0.001$ versus the NC group, $n = 3$. **h** Co-IP results showed that YAP can combine with 14-3-3ζ in renal tubular epithelial cells.

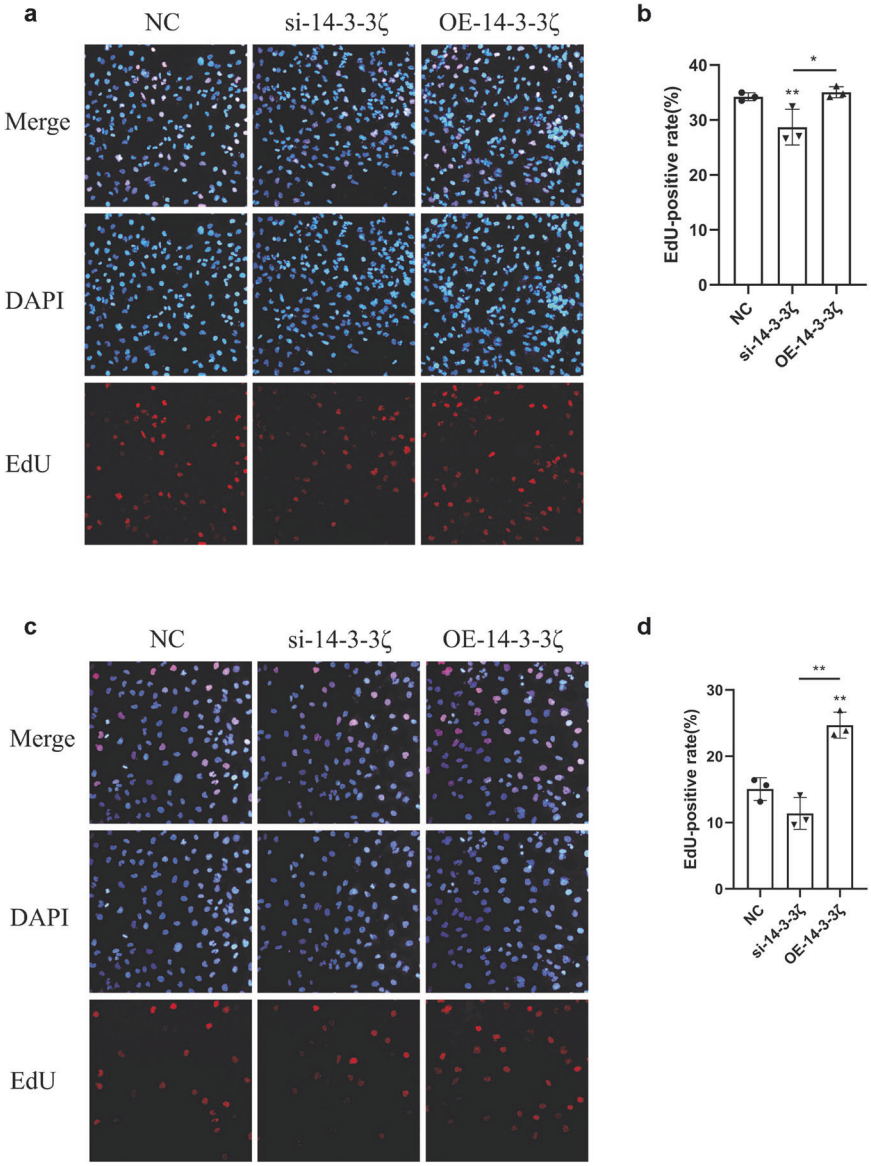

Fig. 3 The proliferation of HK-2 cells changed after 14-3-3ζ knockdown or overexpression. a, **b** Compared with that of the NC group, the EdU-positive rate of HK-2 cells was lower after 14-3-3ζ knockdown, and the overexpression of 14-3-3ζ did not have a significant effect. $^{*}P < 0.05$ and $^{**}P < 0.01$ versus the NC group, $n = 3$. **c**, **d** Three groups of HK-2 cells were treated with H/R. HK-2 cells overexpressing 14-3-3ζ exhibited more obvious proliferation and repair ability after injury, whereas HK-2 cells with 14-3-3ζ knockdown did not exhibit this ability. $^{**}P < 0.01$ versus the NC group, $n = 3$.

significantly, whereas its downstream factors, such as *Ccn*, *Col1a1* and *Acta*, exhibited marked changes at the mRNA level (Fig. 6d). Western blotting revealed that after UIRI stimulation, the expression of active YAP and the fibrotic marker CTGF, α-SMA and vimentin in the OE-14-3-3ζ group was lower than that in the NC group at the protein level. The expression of the epithelial cell marker protein E-cadherin exhibited the opposite result (Fig. 6e and f).

AKI-CKD model mice belonging to the OE-14-3-3ζ group showed decreased renal fibrosis

With the aggravation of renal fibrosis in AKI-CKD model mice, the kidney tissue volume decreases [26]. We used the method of measuring the longest diameter of the whole kidney to reflect the volume of the kidney. After UIRI, the kidney volume was decreased in both the OE-14-3-3ζ group and the NC group, and the decrease in the NC group was more significant than that in the OE-14-3-3ζ group (Fig. 7a and b). Biochemical tests showed that the serum creatinine level of the AKI-CKD model mice belonging to the NC group was higher than that of the sham group and the OE-14-3-3ζ group. The concentration of serum urea nitrogen in the NC group was also significantly higher than that in the other two groups (Fig. 7c and d). The results from pathological PAS staining, Masson staining and Sirius Red staining showed that the area of fibrosis was lower in the OE-14-3-3ζ group than in the NC group (Fig. 7e–g). The results from immunohistochemical staining showed that active YAP was mainly expressed in damaged renal tubular epithelial cells and that α-SMA was deposited in the intercellular substance of the cortex-medullary junction area, and these findings showed the same quantitative trend as that found by Western blotting analysis (Fig. 7h–j). In summary, the overexpression of 14-3-3ζ

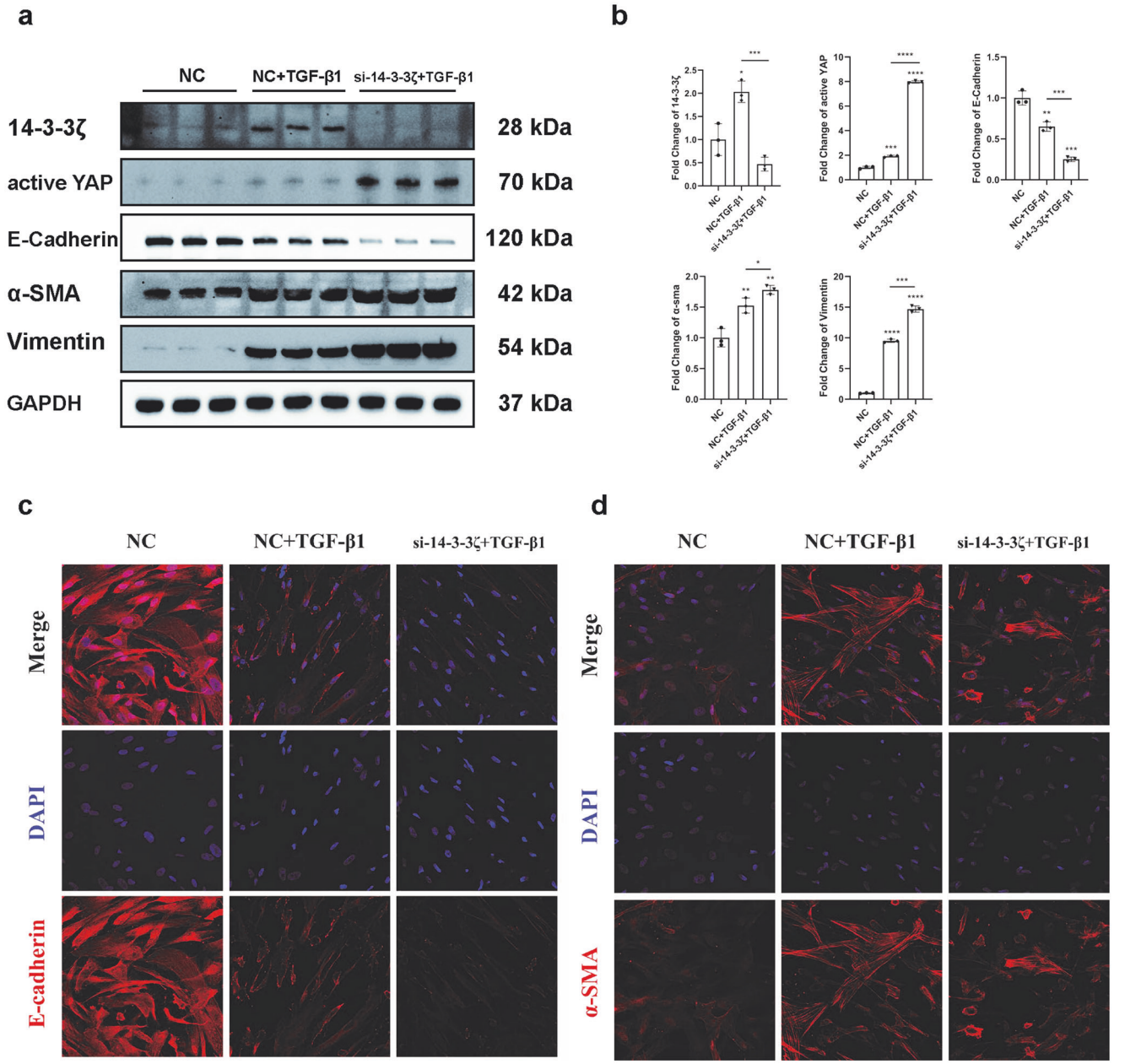

Fig. 4 Fibrosis was aggravated in 14-3-3ζ-knockdown cells treated with TGF-β1 (10 ng/mL). a, **b** The knockdown of 14-3-3ζ significantly increased the expression of active YAP, decreased the expression of the epithelial marker E-cadherin, and increased the expression of fibrotic markers compared with the results found for the NC + TGF-β1 group. $^{*}P < 0.05$, $^{**}P < 0.01$, $^{***}P < 0.001$, and $^{****}P < 0.0001$ versus the NC group, $n = 3$. **c**, **d** The immunofluorescence results are consistent with the Western blot results. 14-3-3ζ knockdown decreased the expression of E-cadherin and increased the expression of α-SMA, ×400.

alleviates nephron fibrogenesis caused by renal ischemia-reperfusion, partially improves kidney function, and protects the kidneys to a certain extent.

DISCUSSION

AKI is a group of clinical syndromes characterized by acute renal dysfunction, and its pathological mechanism involves necrosis of proximal tubular epithelial cells due to ischemia or toxic injury, which results in a sudden decrease in the glomerular filtration rate (GFR) [27]. Injured renal tubules exhibit two outcomes after repair: physiological repair and maladaptive repair. Physiological repair can restore the functions of renal tubules, whereas maladaptive repair leads to fibrosis, causing renal insufficiency and triggering CKD. Renal ischemia-reperfusion can cause acute necrosis of renal tubules, which is a common cause of AKI [28]. Therefore, in this study, the ischemia-reperfusion model was selected as the experimental research model, and the AKI-CKD mouse model was established by unilateral renal vascular clipping and contralateral nephrectomy. The following results were obtained with the overexpression or knockdown of 14-3-3ζ in vitro and in vivo. The overexpression of 14-3-3ζ promoted the phosphorylation of YAP, which resulted in inhibition of the translocation of YAP to the nucleus and reduction of its activation, and a decrease in YAP activation reduced the occurrence and development of renal fibrosis induced by ischemia-reperfusion (Fig. 8). These results are important for identifying key regulatory factors and their regulatory mechanisms in the AKI-CKD transition.

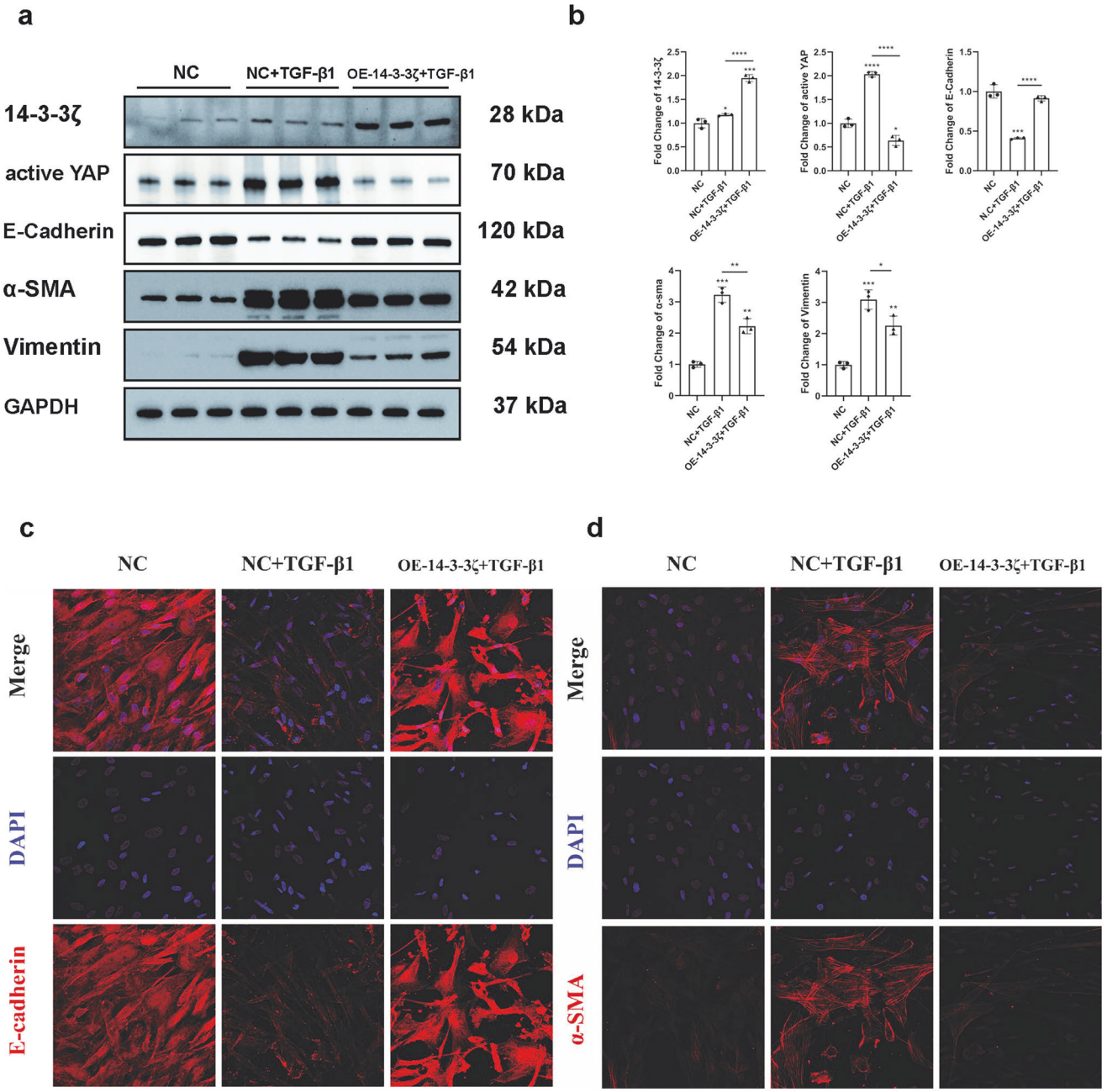

Fig. 5 Fibrosis was relieved in 14-3-3ζ-overexpressing cells treated with TGF-β1 (10 ng/mL). a, **b** Compared with that of the NC + TGF-β1 group, the overexpression of 14-3-3ζ significantly decreased the expression of active YAP, slightly increased the expression of the epithelial marker E-cadherin, and decreased the expression of fibrosis markers. *$P < 0.05$, **$P < 0.01$, ***$P < 0.001$, and ****$P < 0.0001$ versus the NC group, $n = 3$. **c**, **d** The immunofluorescence results are consistent with the Western blot results. 14-3-3ζ overexpression increased the expression of E-cadherin and decreased the expression of α-SMA, ×400.

The mammalian 14-3-3 protein family has seven members: β, ε, γ, η, σ, τ and ζ. The ζ subtype, also known as 14-3-3ζ, is the most abundant in this protein family [29]. The 14-3-3 protein family shows specific binding of phosphopeptides and can act as ligands that easily bind to phosphorylated serine and threonine [30]. As shown in the crystal structure, the 14-3-3 protein family dimer contains two adjacent phosphopeptide binding sites; thus, it can simultaneously bind to two ligands and act as an adaptor to promote the interaction between the target protein and the protein kinase LATS [31, 32]. During transcriptional regulation, transcription factors, as target proteins, can bind to the 14-3-3ζ protein after being phosphorylated [33], and binding to the 14-3-3ζ protein accelerates the phosphorylation of transcription factors [34]. An increasing number of studies have confirmed that 14-3-3ζ plays an important role in the signaling pathway that regulates cell survival. When cells are under unfavorable conditions, such as a hypoxic environment, 14-3-3ζ can promote the activation of survival-related signaling pathways in cells, such as the regulation of cell autophagy, promotion of DNA damage repair, inhibition of cell apoptosis, and protection of cells from stress-induced damage [8, 35–38]. Therefore, we speculate that 14-3-3ζ may inhibit the maladaptive repair of renal tubular epithelial cells.

Previous studies have shown that the expression and activation of the transcriptional coactivator YAP in the renal tubular epithelial

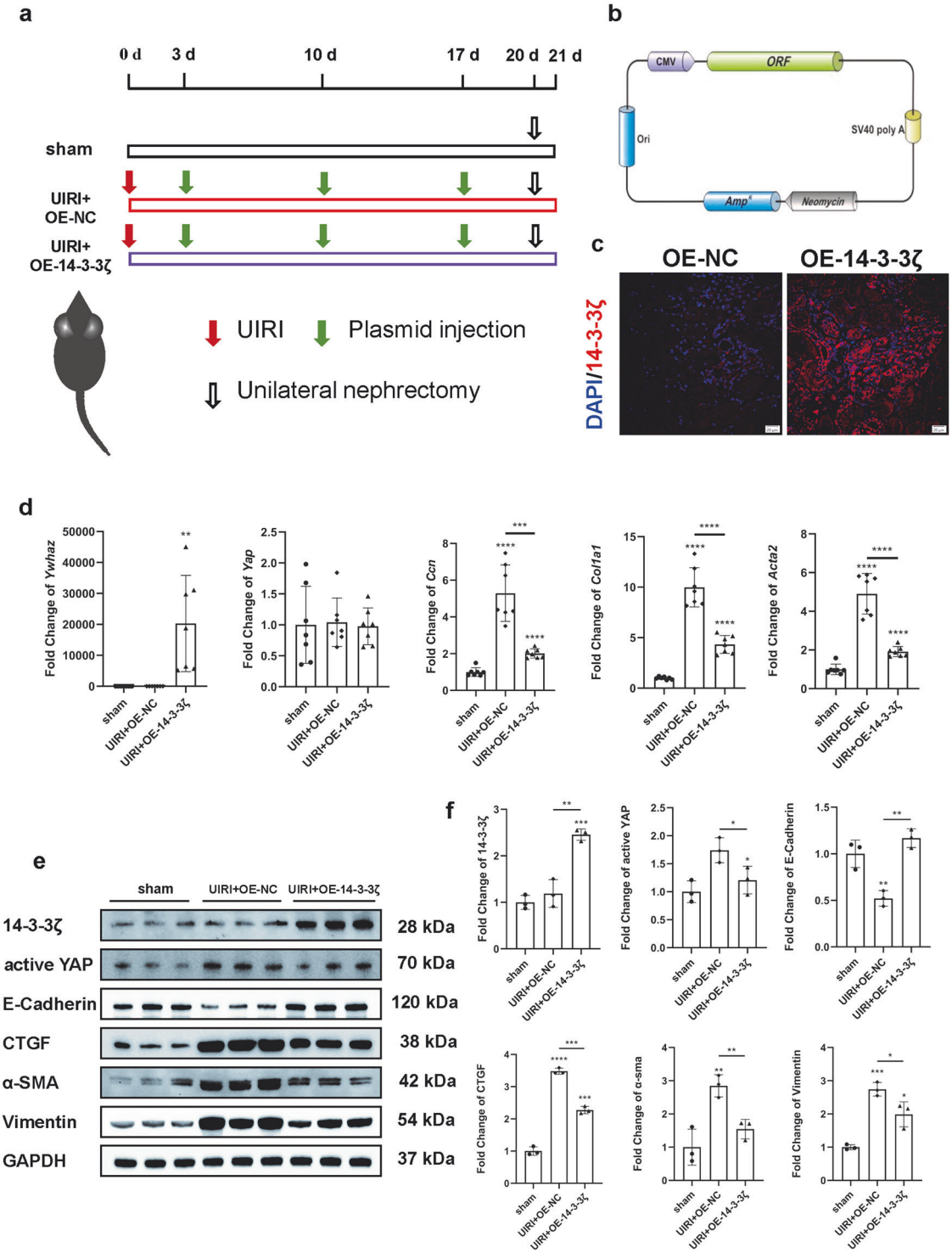

Fig. 6 14-3-3ζ was overexpressed in a mouse model of AKI-CKD via plasmid transfection. a Experimental scheme. The red arrows indicate UIRI, the green arrows indicate the injection of 14-3-3ζ overexpression plasmids or NC plasmids, and the black-edged arrow indicates unilateral nephrectomy the day before tissue collection. **b** Construction of the 14-3-3ζ (Mus) plasmid: The selection marker was resistant to ampicillin, and the size of the complete plasmid was 6561 bp. **c** Immunofluorescence showed the transfection efficiency of 14-3-3ζ overexpression, ×400. **d** Fold change of *Ywhaz*, *Yap*, *Ccn*, *Col1a1*, and *Acta2* at the mRNA level. The differences in fibrotic markers such as *Ccn*, *Col1a1* and *Acta2* between the OE-14-3-3ζ group and NC group were significant, whereas the difference in *Yap* expression was not significant. $^{**}P < 0.01$, $^{***}P < 0.001$, and $^{****}P < 0.0001$ versus the sham group, $n = 7$. **e**, **f** Western blot results showed that the OE-14-3-3ζ group overexpressed 14-3-3ζ and presented lower expression of active YAP and the fibrotic marker CTGF, α-SMA, vimentin but higher expression of the epithelial cell marker protein E-cadherin than the NC group after UIRI. $^{*}P < 0.05$, $^{**}P < 0.01$, $^{***}P < 0.001$, and $^{****}P < 0.0001$ versus the sham group, $n = 3$.

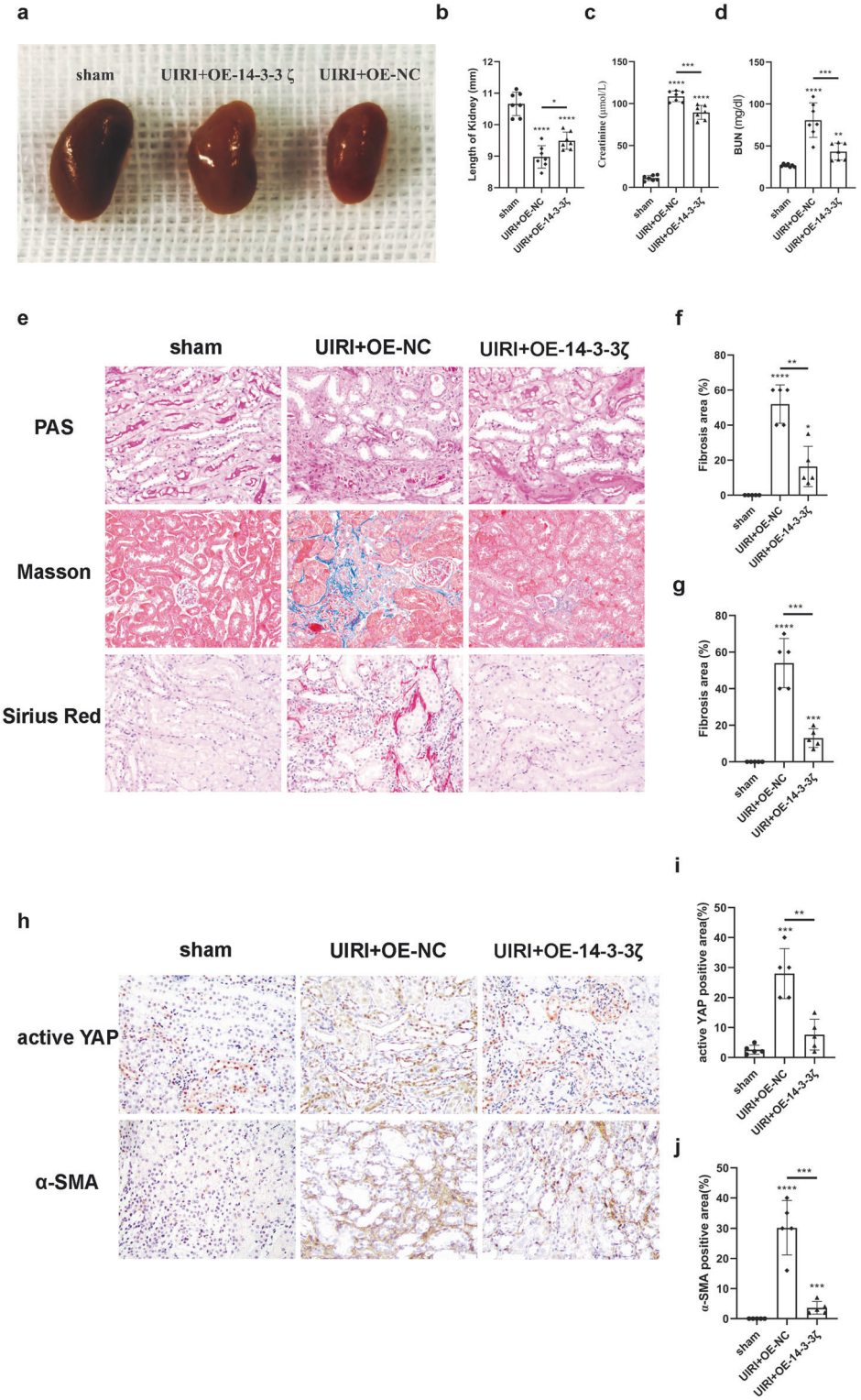

Fig. 7 The levels of serum creatinine and serum urea nitrogen and the degree of fibrosis in the OE-14-3-3ζ model were decreased after UIRI. a, **b** There were differences in the morphology of the kidneys among the different groups. The volumes of the kidneys of the NC group were smaller than those of the sham group, and the longest diameters of the NC group were significantly smaller than those of the sham group. $^{*}P < 0.05$ and $^{****}P < 0.0001$ versus the sham group, $n = 7$. **c**, **d** The serum creatinine concentration and the serum urea nitrogen concentration of the NC group were higher than those of the sham group and the OE-14-3-3ζ group. $^{**}P < 001$, $^{***}P < 0.001$, and $^{****}P < 0.0001$ versus the sham group, $n = 7$. **e**–**g** Fibrosis of the kidney in the OE-14-3-3ζ model was significantly weaker than that in the NC group. $^{*}P < 0.05$, $^{**}P < 0.01$, $^{***}P < 0.001$, and $^{****}P < 0.0001$ versus the sham group, $n = 5$. **h**–**j** The immunohistochemical staining results are consistent with the Western blot results. The expression of active YAP in the OE-14-3-3ζ group was lower than that in the NC group, which mainly had damaged renal tubular epithelial cells, and the expression of α-SMA in the OE-14-3-3ζ group was also lower than that in the NC group; the expression was detected in the cortex medullary junction area. $^{**}P < 0.01$, $^{***}P < 0.001$, and $^{****}P < 0.0001$ versus the sham group, $n = 5$.

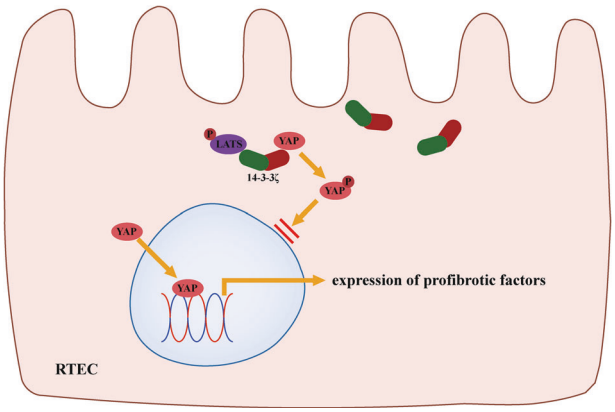

Fig. 8 14-3-3ζ inhibits the expression of profibrotic factors by regulating the phosphorylation of YAP. RTEC, renal tubular epithelial cell; P, phosphorylation.

cells of diabetic patients and diabetic mice are increased. The YAP-dependent paracrine mechanism of proximal renal tubules plays an important role in renal interstitial fibrogenesis caused by diabetes [17]. YAP promotes TGF-β signal transduction by retaining activated Smad2/3 in the nucleus [39]. Moreover, the expression levels of downstream factors such as cyclin E, death-associated inhibitor of apoptosis1 (DIAP1), CTGF and collagen I, III, and IV in the extracellular matrix are upregulated accordingly [40, 41]. The expression of YAP in the cytoplasm and nucleus of renal tubular epithelial cells was significantly increased after AKI. At the AKI stage, this molecule may play a role in promoting cell proliferation and speeding up repair. However, after entering the CKD stage, YAP primarily promotes the activation of fibroblasts and continuous proliferation of renal tubular epithelial cells, resulting in incomplete repair, an abnormally low level of differentiation, and renal fibrosis.

YAP activity can be regulated by phosphorylation. Only when YAP enters the nucleus and binds to TEAD can it play a role in transcriptional regulation. In the cytoplasm, YAP can be phosphorylated by LATS to limit its entry into the nucleus [42]. In this process, 14-3-3ζ plays a role in promoting its phosphorylation. Among the phosphorylation sites of YAP, only Ser127 in humans, Ser112 in mice, as the 14-3-3 protein-binding site, is needed to control the nuclear translocation of YAP [43]. Under physiological conditions, 14-3-3ζ can bind to YAP phosphorylated at Ser127, which silences YAP through its retention in the cytoplasm and thereby inhibits the expression of downstream related factors and maintains the steady state of tissue growth. In this study, the Co-IP results showed that 14-3-3ζ can combine with YAP in renal tubular epithelial cells, and the changes in active YAP and p-YAP that occurred after 14-3-3ζ interference were consistent with the above-described conclusions. Another line of evidence is that the overexpression of 14-3-3ζ in vivo only exerted an effect on YAP at the protein level but not at the mRNA level. 14-3-3ζ most likely regulates the activation of YAP by regulating its phosphorylation. Previous studies have shown that the stimulation of renal tubular epithelial cells by the classic profibrotic factor TGF-β1 can induce the expression of fibrosis-related indicators such as α-SMA and vimentin [44]. The overexpression of 14-3-3ζ inhibited the activation of YAP even though cells were treated with TGF-β1, and the expression of downstream fibrosis-related proteins was also inhibited. In contrast, 14-3-3ζ knockdown aggravated the conversion of TGF-β1-induced cells to a fibrotic phenotype. In vivo, the expression of active YAP in the kidneys of AKI-CKD model mice was higher than that in the kidneys of normal mice from the AKI stage to the CKD stage, whereas the expression of 14-3-3ζ showed a trend of first increasing and then decreasing. We suspect that the occurrence of CKD may be related to a reduced inhibitory effect of 14-3-3ζ on YAP. In subsequent in vivo intervention experiments, we used plasmid transfection technology to overexpress 14-3-3ζ in mice. After ischemia-reperfusion stimulation, the OE-14-3-3ζ group showed amelioration of the changes in serum creatinine, serum urea nitrogen and renal fibrosis, and the expression of fibrotic markers was also lower than that in the NC group. These findings suggested that 14-3-3ζ may affect the repair process of renal tubular epithelial cells after injury by regulating the activation of YAP, inhibiting fibrosis, and promoting physiological repair.

According to current research, 14-3-3ζ shows potential in disease treatment. The adenovirus-mediated transfection of CIA mice with 14-3-3ζ stops the progression of arthritis and inhibits the expression of proinflammatory cytokines in joint tissues, lymph nodes and spleen. This result suggests that 14-3-3ζ is an excellent target in rheumatoid arthritis (RA) treatment [45]. With respect to kidney disease, studies have reported that 14-3-3ζ can promote the repair of the human renal tubular epithelial cell line HK-2 after cisplatin-induced damage [46]. 14-3-3ζ can promote the repair of renal tubular epithelial cells and protect cells in unfavorable environments. In this study, 14-3-3ζ showed a trend of increased expression at the AKI stage, whereas PCNA expression was also significantly increased, and these two factors showed colocalization. 14-3-3ζ may result in a synergistic effect to promote repair at this stage. This study mainly explored the role of 14-3-3ζ in inhibiting fibril formation in the CKD stage, but the promotion of cell proliferation and repair was not involved. This limitation undoubtedly provides a direction for future research.

In summary, 14-3-3ζ reduced the degree of fibrosis by regulating the activity of the transcriptional coactivator YAP during renal fibrosis and retarded the AKI-CKD transition process caused by ischemia-reperfusion injury. The above-described research results may provide ideas for the prevention and treatment of the AKI-CKD transition.

ACKNOWLEDGEMENTS

This work was supported by the National Key R&D Program of China (2017YFA0103200, 2017YFA0103203) and the National Natural Science Foundation of China (No. 82030025, 81830060).

AUTHOR CONTRIBUTIONS

XMC, LQW and LSZ designed the study; TTW, LLW, WJS, YHZ, JNL, BF, and XW carried out experiments; TTW drafted the paper; LLW, JW, LSZ, QGL and XYB revised the paper; all authors approved the final version of the manuscript.

ADDITIONAL INFORMATION

Supplementary information The online version contains supplementary material available at https://doi.org/10.1038/s41401-022-00946-y.

Competing interests: The authors declare no competing interests.

REFERENCES

1. Molitoris BA. Therapeutic translation in acute kidney injury: the epithelial/endothelial axis. J Clin Invest. 2014;124:2355–63.
2. Al-Jaghbeer M, Dealmeida D, Bilderback A, Ambrosino R, Kellum JA. Clinical decision support for in-hospital AKI. J Am Soc Nephrol. 2018;29:654–60.
3. Hoste EA, Bagshaw SM, Bellomo R, Cely CM, Colman R, Cruz DN, et al. Epidemiology of acute kidney injury in critically ill patients: the multinational AKI-EPI study. Intensive Care Med. 2015;41:1411–23.
4. Coca SG, Singanamala S, Parikh CR. Chronic kidney disease after acute kidney injury: a systematic review and meta-analysis. Kidney Int. 2012;81:442–8.
5. Hsu CY. Yes, AKI truly leads to CKD. J Am Soc Nephrol. 2012;23:967–9.
6. James MT, Bhatt M, Pannu N, Tonelli M. Long-term outcomes of acute kidney injury and strategies for improved care. Nat Rev Nephrol. 2020;16:193–205.
7. Venkatachalam MA, Weinberg JM, Kriz W, Bidani AK. Failed Tubule Recovery, AKI-CKD transition, and kidney disease progression. J Am Soc Nephrol. 2015; 26:1765–76.

8. Zhao L, Han F, Wang J, Chen J. Current understanding of the administration of mesenchymal stem cells in acute kidney injury to chronic kidney disease transition: a review with a focus on preclinical models. Stem Cell Res Ther. 2019;10:385.
9. Yang L, Besschetnova TY, Brooks CR, Shah JV, Bonventre JV. Epithelial cell cycle arrest in G2/M mediates kidney fibrosis after injury. Nat Med. 2010;16:535–43.
10. Chen J, You H, Li Y, Xu Y, He Q, Harris RC. EGF receptor-dependent YAP activation is important for renal recovery from AKI. J Am Soc Nephrol. 2018;29:2372–85.
11. Rausch V, Hansen CG. The Hippo Pathway, YAP/TAZ, and the plasma membrane. Trends Cell Biol. 2020;30:32–48.
12. Zhu C, Tabas I, Schwabe RF, Pajvani UB. Maladaptive regeneration - the reawakening of developmental pathways in NASH and fibrosis. Nat Rev Gastroenterol Hepatol. 2021;18:131–42.
13. Zhang T, He X, Caldwell L, Goru SK, Ulloa Severino L, Tolosa MF, et al. NUAK1 promotes organ fibrosis via YAP and TGF-β/SMAD signaling. Sci Transl Med. 2022;14:eaaz4028.
14. Anorga S, Overstreet JM, Falke LL, Tang J, Goldschmeding RG, Higgins PJ, et al. Deregulation of Hippo-TAZ pathway during renal injury confers a fibrotic maladaptive phenotype. FASEB J. 2018;32:2644–57.
15. He X, Tolosa MF, Zhang T, Goru SK, Ulloa Severino L, Misra PS, et al. Myofibroblast YAP/TAZ activation is a key step in organ fibrogenesis. JCI Insight. 2022;7:e146243.
16. Liang M, Yu M, Xia R, Song K, Wang J, Luo J, et al. Yap/Taz deletion in Gli(+) cell-derived myofibroblasts attenuates fibrosis. J Am Soc Nephrol. 2017;28:3278–90.
17. Chen J, Wang X, He Q, Bulus N, Fogo AB, Zhang MZ, et al. YAP activation in renal proximal tubule cells drives diabetic renal interstitial fibrogenesis. Diabetes. 2020;69:2446–57.
18. Zhang B, Shi Y, Gong A, Pan Z, Shi H, Yang H, et al. HucMSC exosome-delivered 14-3-3zeta orchestrates self-control of the wnt response via modulation of YAP during cutaneous regeneration. Stem Cells. 2016;34:2485–500.
19. Zhu H, Liao J, Zhou X, Hong X, Song D, Hou FF, et al. Tenascin-C promotes acute kidney injury to chronic kidney disease progression by impairing tubular integrity via αvβ6 integrin signaling. Kidney Int. 2020;97:1017–31.
20. Skrypnyk NI, Harris RC, de Caestecker MP. Ischemia-reperfusion model of acute kidney injury and post injury fibrosis in mice. J Vis Exp. 2013:50495. https://doi.org/10.3791/50495.
21. Zhou D, Li Y, Zhou L, Tan RJ, Xiao L, Liang M, et al. Sonic hedgehog is a novel tubule-derived growth factor for interstitial fibroblasts after kidney injury. J Am Soc Nephrol. 2014;25:2187–200.
22. Liu F, Song Y, Liu D. Hydrodynamics-based transfection in animals by systemic administration of plasmid DNA. Gene Ther. 1999;6:1258–66.
23. Tajima T, Yoshifuji A, Matsui A, Itoh T, Uchiyama K, Kanda T, et al. beta-hydroxybutyrate attenuates renal ischemia-reperfusion injury through its anti-pyroptotic effects. Kidney Int. 2019;95:1120–37.
24. Melnikov VY, Ecder T, Fantuzzi G, Siegmund B, Lucia MS, Dinarello CA, et al. Impaired IL-18 processing protects caspase-1-deficient mice from ischemic acute renal failure. J Clin Invest. 2001;107:1145–52.
25. Brennan EP, Nolan KA, Börgeson E, Gough OS, McEvoy CM, Docherty NG, et al. Lipoxins attenuate renal fibrosis by inducing let-7c and suppressing TGFβR1. J Am Soc Nephrol. 2013;24:627–37.
26. Thorenz A, Derlin K, Schroder C, Dressler L, Vijayan V, Pradhan P, et al. Enhanced activation of interleukin-10, heme oxygenase-1, and AKT in C5aR2-deficient mice is associated with protection from ischemia reperfusion injury-induced inflammation and fibrosis. Kidney Int. 2018;94:741–55.
27. Du T, Zhu YJ. The regulation of inflammatory mediators in acute kidney injury via exogenous mesenchymal stem cells. Mediators Inflamm. 2014;2014:261697.
28. Del Re DP, Yang Y, Nakano N, Cho J, Zhai P, Yamamoto T, et al. Yes-associated protein isoform 1 (Yap1) promotes cardiomyocyte survival and growth to protect against myocardial ischemic injury. J Biol Chem. 2013;288:3977–88.
29. Londhe AD, Bergeron A, Curley SM, Zhang F, Rivera KD, Kannan A, et al. Regulation of PTP1B activation through disruption of redox-complex formation. Nat Chem Biol. 2020;16:122–5.
30. Reinhardt HC, Yaffe MB. Phospho-Ser/Thr-binding domains: navigating the cell cycle and DNA damage response. Nat Rev Mol Cell Biol. 2013;14:563–80.
31. Zha J, Harada H, Yang E, Jockel J, Korsmeyer SJ. Serine phosphorylation of death agonist BAD in response to survival factor results in binding to 14-3-3 not BCL-X(L). Cell. 1996;87:619–28.
32. Yaffe MB, Rittinger K, Volinia S, Caron PR, Aitken A, Leffers H, et al. The structural basis for 14-3-3:phosphopeptide binding specificity. Cell. 1997;91:961–71.
33. Brunet A, Bonni A, Zigmond MJ, Lin MZ, Juo P, Hu LS, et al. Akt promotes cell survival by phosphorylating and inhibiting a Forkhead transcription factor. Cell. 1999;96:857–68.
34. Brunet A, Kanai F, Stehn J, Xu J, Sarbassova D, Frangioni JV, et al. 14-3-3 transits to the nucleus and participates in dynamic nucleocytoplasmic transport. J Cell Biol. 2002;156:817–28.
35. Medina A, Ghahary A. Transdifferentiated circulating monocytes release exosomes containing 14-3-3 proteins with matrix metalloproteinase-1 stimulating effect for dermal fibroblasts. Wound Repair Regen. 2010;18:245–53.
36. Pozuelo-Rubio M. Regulation of autophagic activity by 14-3-3zeta proteins associated with class III phosphatidylinositol-3-kinase. Cell Death Differ. 2011;18:479–92.
37. Pozuelo-Rubio M. 14-3-3 proteins are regulators of autophagy. Cells. 2012;1:754–73.
38. Zannis-Hadjopoulos M, Yahyaoui W, Callejo M. 14-3-3 cruciform-binding proteins as regulators of eukaryotic DNA replication. Trends Biochem Sci. 2008;33:44–50.
39. Szeto SG, Narimatsu M, Lu M, He X, Sidiqi AM, Tolosa MF, et al. YAP/TAZ are mechanoregulators of TGF-β-Smad signaling and renal fibrogenesis. J Am Soc Nephrol. 2016;27:3117–28.
40. Iwakura T, Fujigaki Y, Fujikura T, Tsuji T, Ohashi N, Kato A, et al. Cytoresistance after acute kidney injury is limited to the recovery period of proximal tubule integrity and possibly involves Hippo-YAP signaling. Physiol Rep. 2017;5:e13310.
41. Xu J, Li PX, Wu J, Gao YJ, Yin MX, Lin Y, et al. Involvement of the Hippo pathway in regeneration and fibrogenesis after ischaemic acute kidney injury: YAP is the key effector. Clin Sci. 2016;130:349–63.
42. Lei QY, Zhang H, Zhao B, Zha ZY, Bai F, Pei XH, et al. TAZ promotes cell proliferation and epithelial-mesenchymal transition and is inhibited by the hippo pathway. Mol Cell Biol. 2008;28:2426–36.
43. Chen Q, Zhang N, Xie R, Wang W, Cai J, Choi KS, et al. Homeostatic control of Hippo signaling activity revealed by an endogenous activating mutation in YAP. Genes Dev. 2015;29:1285–97.
44. Gewin L, Zent R. How does TGF-β mediate tubulointerstitial fibrosis? Semin Nephrol. 2012;32:228–35.
45. Kong JS, Park JH, Yoo SA, Kim KM, Bae YJ, Park YJ, et al. Dynamic transcriptome analysis unveils key proresolving factors of chronic inflammatory arthritis. J Clin Invest. 2020;130:3974–86.
46. Wang J, Jia H, Zhang B, Yin L, Mao F, Yu J, et al. HucMSC exosome-transported 14-3-3ζ prevents the injury of cisplatin to HK-2 cells by inducing autophagy in vitro. Cytotherapy. 2018;20:29–44.